Correlation of micro and nano-scale defects with WVTR for aluminium oxide barrier coatings for flexible photovoltaic modules

L. Blunt*, M. Elrawemi, L. Fleming and F. Sweeney

Department of Mechanical Engineering,
Centre for Precision Technologies,
University of Huddersfield,
HD1 3DH, Huddersfield, UK
E-mail: l.a.blunt@hud.ac.uk
E-mail: Mohamed. Elrawemi@hud.ac.uk
E-mail: l.t.fleming@hud.ac.uk
E-mail: f.sweeney@hud.ac.uk
*Corresponding author

Abstract: This paper seeks to establish a correlation between surface topographical defects and Water Vapour Transmission Rate (WVTR) measured under laboratory conditions for aluminium-oxide (Al_2O_3) barrier film employed in flexible photovoltaic (PV) modules. Defects in the barrier layers of PV modules causing high WVTR are not well characterised and understood. A WVTR of ~10^{-1} g/m^2/day is sufficient for the most packaging applications, but ≤10^{-6} g/m^2/day is required for the encapsulation of long-life flexible PV modules (Carcia et al., 2010a, 2010b). In this study, Surface metrology techniques along with Scanning Electron Microscopy (SEM) were used for a quantitative characterisation of the barrier film defects. The investigation have provided clear evidence for the correlation of surface defect density and the transmission of water vapour through the barrier coating layer. The outcomes would appear to suggest that small numbers of large defects are the dominant factor in determining WVTR for these barrier layers.

Keywords: photovoltaics; micro; nano-defects; aluminium oxide; WVTR; water vapour transmission rate.

Reference to this paper should be made as follows: Blunt, L., Elrawemi, M., Fleming, L. and Sweeney, F. (2013) 'Correlation of micro and nano-scale defects with WVTR for aluminium oxide barrier coatings for flexible photovoltaic modules', *Int. J. Precision Technology*, Vol. 3, No. 3, pp.290–302.

Biographical notes: L. Blunt has an honours degree in Materials Technology and a PhD in "The Metallurgy of Centreless Ground Surfaces" at Coventry University. He has formed extensive industrial collaborations in particular with Taylor Hobson Ltd a world leading metrology company. He is now the Director of the Centre for Precision Technologies. His research specialises in the applications of surface metrology to new production processes.

M. Elrawemi is a PhD researcher student, University of Huddersfield, UK. He received the Master Degree in 2010 in the field of mechanical engineering design.

L. Fleming is a Senior Lecturer and Researcher in The School of Computing and Engineering at The University of Huddersfield, her research is mainly focussed on the application of surface metrology to novel situations with an emphasis on improvements in engineering function and performance.

F. Sweeney is a Post-Doctoral Researcher in the School of Computing and Engineering at the University of Huddersfield. He gained his PhD from the University of Strathclyde in 2005 in "Characterisation of Nitride Thin Films by Electron Backscattered Diffraction Correlated with Cathodoluminescence Spectroscopy and Imaging". In 2007 he moved to the University of Sheffield where he was involved in the development of electron ptychography in the Transmission Electron Microscopy. Currently, the main focus of his research at Huddersfield is the characterisation of the structure and morphology of materials by electron microscopy and associated techniques.

1 Introduction

The lifetime and reliability of photovoltaic modules is influenced by defects within layers making up the PV modules. These defects have their origins either in manufacturing processes or in operational exposure (Sander et al., 2010). The state-of-the-art flexible PV film technologies have efficiencies at or beyond the level of Si-based rigid PV modules as high as 19.9% currently in use are those based on the material $CuIn_{1-x}Ga_xSe_2$ (Jackson et al., 2011). These flexible technologies offer advantages in architectural design for Building-Integrated-Photovoltaic (BIPV) as well as flat plate module applications. The lifetime of flexible multi-layer CIGS solar technology has always been one of the biggest challenges, as it can be influenced by moisture permeating through defects in the coatings of the protective barrier films and compromising the efficiency of the modules. Therefore, in order for this technology to satisfy the international standard (IEC 61646), which requires that the efficiency does not degrade below 100% after 1000 hours in an environment of 85°C and 85% relative humidity (RH), the modules must be must be effectively encapsulated (Olsen, 2010).

Detection and characterisation of PV barrier film defects is necessary for manufactures to assure their function and to improve the manufacturing process and to aid in product development. Therefore, in order to determine which features in the barrier coating have an effect on the overall efficiency, these features must be detected and characterized and then correlated with the layer function. Various researchers have presented methods for non- destructive defect detection for PV modules. Rueland et al. (2005) proposed a technique to detect cracks by transmitting a high intensity flashlight through the PV films, capturing the image with a CCD camera fixed to an optical filter. The light intensity is then directly correlated with the thickness of film material. Hence, by identifying bright areas in the images, defects down to approximately 5 μm width in the film analysed. However, Belyaev et al. (2006) proposed an experimental methodology using a Resonance Ultrasonic Vibrations (RUV) system to detect cracks in PV substrates. This technique enabled fast data acquisition and analyses matching the throughput of solar cell production lines and capable of non-destructively detecting

millimetre length cracks. Hilmersson (2006) detected cracks in PV films using a vibration method in the form of an impact test as a non-destructive way. This technique can detect cracks with lengths of ≥100 µm. However, the major disadvantage is the time required to test the wafer (it takes 5–10 seconds to inspect a 100 mm by 100 mm wafer). Moreover, Connor et al. (1998) proposed Scanning Acoustic Microscopy (SAM) technique to be used as a method of determining the presence of cracks, though this method is not feasible during the mass production of PV cells. This method showed its limitation since the time required to scan a 100 mm by 100 mm wafer was between 10–15 minutes. The SAM method, however, did allow for cracks ≥5 µm in length to be detected. Rakotoniaina et al. (2004) employed an Ultrasound Lock-in Thermography (ULT) method to detect cracks in PV modules. This method can detect cracks with lengths ≥100 µm and it takes around 5–10 seconds to inspect a 100 mm by 100 mm film. While more than a couple of seconds are accepted for quality control, this long acquisition time makes ULT unsuitable for in-line detection. Florin and Costin (2011) detected and analysed accumulated particles over different PV surfaces using infrared (IR) thermography method. Their results indicated that the IR method can be effectively utilised for detection of defects as small as a few millimetres in a very short time of about 1 second.

The literature review has confirmed that all the previous described techniques cannot be employed to detect micro (<5 µm) and nano-scale defects such as pinholes, small particles and micro-cracks in the Al_2O_3 barrier layer and they face the challenge of speed vs. resolution. Hence, to go beyond these limitations surface metrology and scanning microscopy techniques will be used in this study as non-destructive tools to detect defects of down to approximately 1 nm in vertical and lateral resolution.

2 Design of flexible PV module

Figure 1 shows a schematic view of the functional layer order in flexible CIGS PV modules. CIGS (Cu In_x Ga $_{(1-x)}$ Se_2) is a semiconductor where the value of x can vary from 1 (pure Copper Indium Selenide) to 0 (pure Copper Gallium Selenide), and it is mainly used in the form of polycrystalline thin films. Prior to the final encapsulation, these cells are only 2–10 µm thick. They are prepared from a number of micrometre thin layers, each layer with specific thickness ranging from 0.15–1.8 µm. These flexible devices are fabricated on polymer film by the repeated deposition, and patterning, of thin layer materials using roll-to-roll technology (Søndergaard et al., 2011).

Long-term performance reliability of CIGS PV modules is highly important to their success in gaining broad market acceptance. Encapsulation capable of blocking or minimizing moisture ingress is therefore essential for PV modules to protect the absorber CIGS layer. Studies regarding the encapsulation technologies have been carried out by Carcia et al. (2010a, 2010b), the authors compared the moisture sensitivity of CIGS cell protected by 55 nm thick Al_2O_3 film, grown by ALD techniques, with equivalent CIGS cells protected with a rigid glass layer, and with a PolyEthylene Terephthalate (PET) film. The study continued for more than 1000 hours at 85°C and 85%RH, with simulated solar illumination. The CIGS cell protected with the PET layer lost about half its efficiency (12.5–6.6%) after ageing for 1020 h (42.5 days) at 85°C and 85%RH, whereas

the CIGS cell protected with the 55 nm ALD Al_2O_3 barrier film and the cell with a glass layer showed only small net change (<3%) in efficiency. However, the authors did not identify and conclude the reasons behind this degradation in the modules efficiency. Hence in order to understand the factors affecting the efficiency and the lifespan of PV modules, a correlation needs to be established between film defects and WVTR measured under laboratory conditions. This paper reports result of surface measurements conducted to characterise uncoated and barrier (Al_2O_3 ALD) coated polymer films. The surface topography is assessed using the latest advanced surface metrology instruments and the latest segmentation feature parameter analysis (ISO 25178-pt2, 2012). The presence of the defects is then correlated with the Water Vapour Transmission Rate (WVTR) as measured on representative sets of films using Isostatic (MOCON) standard test (Duncan et al., 2005).

Figure 1 Schematic of the flexible PV module (Courtesy of Flisom, Switzerland) (see online version for colours)

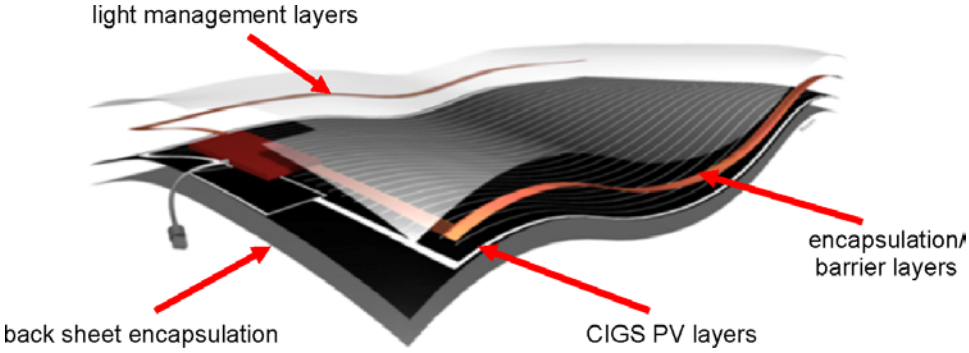

3 Experimental procedure

3.1 Test specimen fabrication

A set of four 80 mm diameter samples coated with 40 nm of Al_2O_3 using ALD techniques were assessed, along with a non-coated substrate. The ALD technique is a controlled layer-by-layer deposition that enables the deposition of thin, smooth, and highly conformal films with atomic layer precision and their functional thickness is determined by the number of cycles and varies roughly from 1 nm to 100 nm (Thein, 2006). The ALD for a 40 nm film thickness is approx. 290 cycles. The film substrate used in this study is PolyEthylene Naphthalate (PEN) material; where the thickness of this substrate is specified to be 125 µm. This polymer film must be of very high quality in order to avoid creating defects. There is a thin layer on top of the PEN made from the same materials, 3–4 µm thick, which the vendor applies to the surface to planarise the pits and spikes in the device layers. The 40 nm thick ALD Al_2O_3 is incorporated on top of the planarised layer as shown in Figure 2.

Figure 2 Schematic cross-section of CIGS PV cell (Courtesy of Flisom, Switzerland) (see online version for colours)

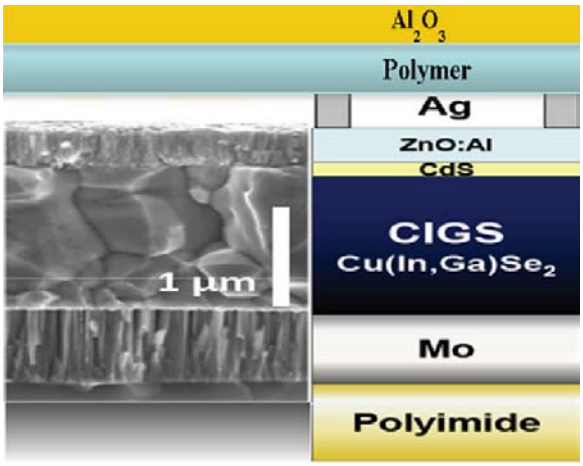

3.2 Exposure

All the coated samples are measured for WVTR using Isostatic standard test (MOCON) instrumentation prior to the surface measurements. This method involves the test specimen being held such that it separates two sides of a test chamber as shown in Figure 3. One side of the sample, the 'wet side', is exposed to the gas or vapour to be studied; this can be done statically or with a continuous stream of permeate gas to maintain a constant pressure concentration. On the detector side, the 'dry side', the sample is subjected to a zero relative humidity, the permeating gas or vapour is swept away with a carrier gas (usually nitrogen) and fed into a sensor/detector usually infrared. The detector is often specific to the permeating types (Duncan et al., 2005).

Figure 3 WVTR test using an infrared detection technique (see online version for colours)

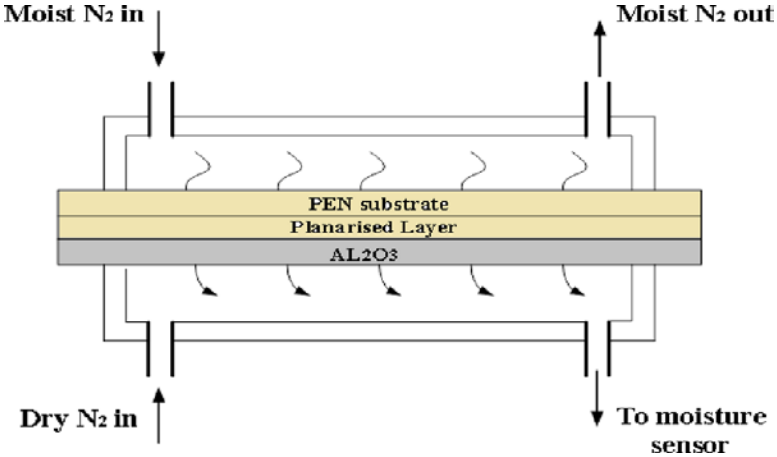

3.3 Water vapour permeation theory

The permeability of the film is determined from the amount or rate of permeation and experimental parameters such as time, sample area, sample thickness, pressure differences, concentrations, temperature etc. Assuming Fickian diffusivity (i.e., diffusivity is independent of concentration), the transient WVTR can be described by the following equation (Kempe, 2006).

$$\mathrm{WVTR} = \frac{DC_{\mathrm{sat}}}{l}\left(1 + 2\sum_{n=1}^{\infty}(-1)^n \mathrm{e}^{\frac{-Dn^2\pi^2 t}{l^2}}\right) \tag{1}$$

where D is the diffusivity (cm^2/s) and it is determined by the time required to reach steady state, after which the water saturation concentration was determined by steady-state WVTR; l is the sample thickness (mm); t is elapsed time (h), and C_{sat} ($\mathrm{g/cm}^3$) is the concentration of water at saturation.

In this study, the WVTR test was conducted at relative humidity 90% and temperature of 38°C at specified time using Isostatic standard test instrumentation (MOCON). The WVTR values are shown in Table 1.

Table 1 Water Vapour Transmission Rate at specified conditions 38°C and 90% RH

Sample No.	*Water Vapour Transmission Rate* ($\mathrm{g/m}^2$/24 h)	*Stabilisation time* (days)
1	1.1×10^{-3}	11
2	1.3×10^{-3}	11
3	4.1×10^{-3}	5
4	2.0×10^{-3}	5

The results show that sample 3 had the highest WVTR. This study's hypothesis is that the presence of micro/nanoscale defects, (size and distribution) might play a critical role in determining WVTR.

4 Defect detection methodology

Since defects in the barrier film of the PV module are expected to seriously reduce their conversion efficiency and usable lifespan, the inspection and understanding of the functional significance of these defects is a very important aspect for the development of both the product and the manufacturing process. In this study, surface metrology techniques particularly optical microscopy, Coherence Correlation Interferometry (CCI) and Scanning Electron Microscopy (SEM) were used to measure the previously tested samples.

4.1 Optical microscopy

A Keyence VHX-600 digital HD CCD microscope, equipped with 20 to 200x objective lenses was primarily utilised in a clean room environment for initial characterisation of the samples. The investigation shows that, different types of features were noted on each

sample; these features are different in terms of their type, width and height. A typical example of these features is shown in Figure 4. The figure shows a pit type feature which has allowed the water vapour to permeate through the barrier causing delamination of the Al_2O_3 layer from the planarised polymer layer.

Figure 4 Form and scale of large defect feature (see online version for colours)

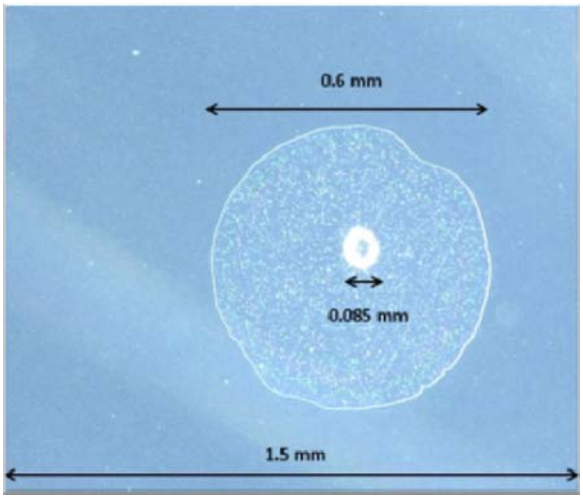

4.2 White light scanning optical interferometry

The recording of the size scale of the features observed from the previous survey using the optical microscope was completed using White Light Scanning Interferometry (WLSI). This method was used to carry out 3D surface analysis, and provides a number of important parameters; including surface roughness, feature height and width. These parameters could possibly have a large influence upon the efficiency of the PV barrier layer (Conroy, 2012). The WLSI instrument used in this study was the Ametek Taylor Hobson CCI 6000 (Coherence Correlation Interferometer). The instrument has been calibrated according to its manufacture specifications and was used in a clean room environment to avoid any possible damage and contamination of the samples. A 20× objective lens was used; this lens gave a measurement area of roughly 1 mm^2 and a potential vertical resolution of about 0.1 nm with lateral resolution of approximately 0.88 μm. In this work which follows, it was considered important to identify the surface topography features in the Al_2O_3 layer as these were thought to be directly contributed to the WVTR value. Cataloguing and determining the significance of these features, and measuring their size, distribution, area and volume as well as the ability to classify these features and determine correlation with WVTR, is being considered as a basis for developing a suitable in-line defect detection system. All Al_2O_3 samples including the uncoated substrate were measured using the WLSI technique. 700 measurements, equating to 14% of the total surface area of all the specimens was measured. The measurements showed the Al_2O_3 barrier layer has many features; these features varied from one sample to another. Table 2 catalogues the observed features and their size scale and Figure 5(a) and (b) shows typical examples of these defects as characterised by WLSI.

The surface roughness of defect free sample areas was ~0.6 nm. Areal surface texture topography analysis was carried out using the feature parameter set (ISO 25178-pt2, 2012; Jiang et al., 2011). Standard characterisation techniques are not robust enough to isolate outliers and to distinguish between the significant and insignificant defects. Therefore standard approaches do not clearly differentiate between the most defective and non-defective samples. Table 3 shows the mean value of the roughness average for each sample (700 measurements).

Table 2 Types of defects and their size scale

Type of defect	*Feature size*	
	Height/depth	*Width*
Spikes	≥3x Sq. height	≤3 µm (~3 sample spacings)
Cracks	≥3x Sq. depth	≥300 µm length (1/3 field of view)
Scratches	≥3x Sq. height	≥300 µm length (1/3 field of view)
Ghost defects (unmeasurable feature)	Not measurable	≥3 µm width
Pinholes	≥3x Sq. depth	≤3 µm lateral dimension
Peaks	≥3 x Sq. height	≥3 µm width
Holes	≥3x Sq. depth	≥3 µm lateral dimension

Figure 5 Two typical types of defects: (a) 'crack' type defect and (b) 'hole' type defect (see online version for colours)

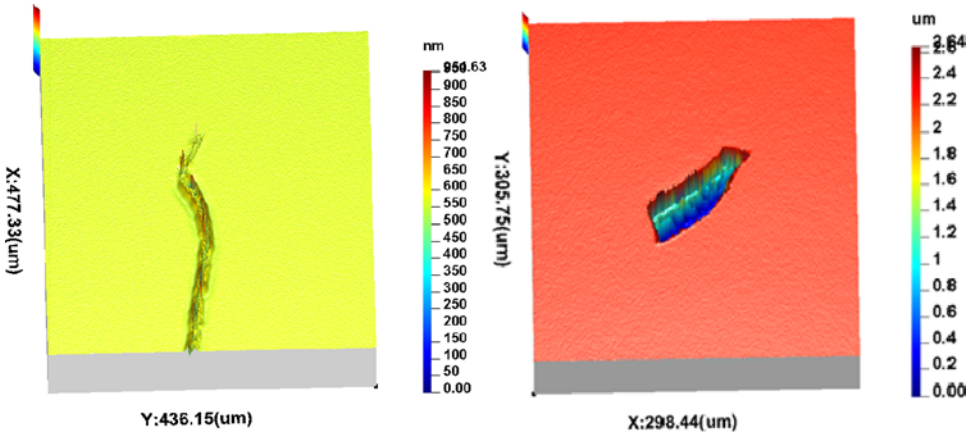

(a) (b)

Table 3 S_a parameters mean value

Sample No.	*S_a parameters mean value* (nm)
Sample 1	0.88
Sample 2	0.80
Sample 3	0.78
Sample 4	0.87
Uncoated/Sample	1.0

The parameter S_q (RMS Roughness) indicated that, sample 3 has more large defects than the other characterised samples as it has the highest standard deviation variation (7.4 nm < S_q < 96 nm) due to the existence of large defects on the samples surface (Figure 6).

Figure 6 Standard deviation averages (see online version for colours)

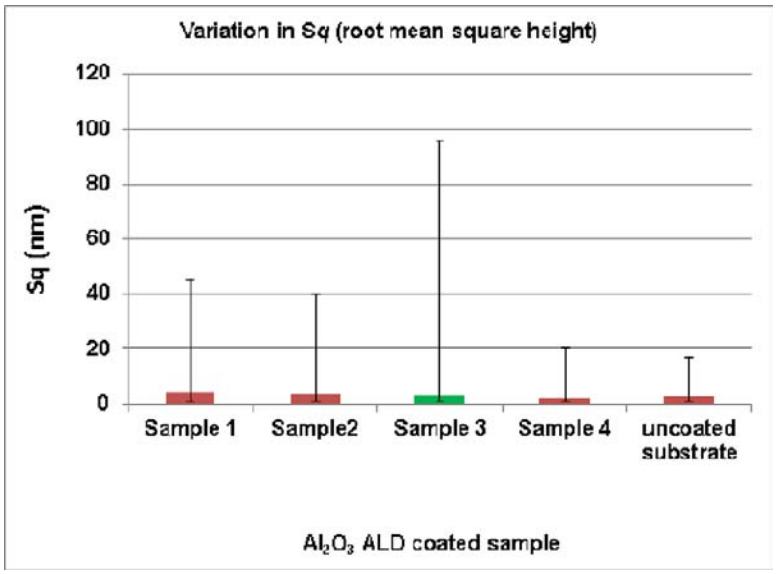

Following initial topography analysis a method of 'Wolf pruning' (ISO 25178-pt2, 2012) was utilised to carry out topography segmentation. The method provides a reliable approach for extracting features of functional interest and by accurately excluding insignificant geometrical features that are induced, such as measurement noise. The procedure consists of finding the peak or pit(dale) with the smallest height difference and combining it with the adjacent topographical saddle point, where the threshold can be selected to give pruning of only those peak and dale features that are greater than 20% of the maximum peak to valley magnitude (S_z) is undertaken. The result of this is to leave only those peaks and dales that are deemed to be significant in the resultant three dimensional output data. This 'toolbox' method was adapted to automatically detect significant hills and dales features. In this procedure a parameter S*fd* (where S*fd* = the number of significant hills + significant dales) was used to define the significance of any peak/pit greater than 20% of the total peak to valley roughness (S_z). Using this default significance value for the defects, the results showed no clear correlation with the WVTR results as shown in Figure 7(a).

A further analysis conducted with additional prune conditions on sample 3 (highest WVTR value) and sample 4 (lower WVTR value) is shown in Figure 7(b). In this case additional lateral dimension criteria were introduced in order to isolate only the largest defects. Based on the visual assessment, the criteria of being assigned as a large defects was (6σ where (S_q = 0.6 nm) height) and 15 µm diameter were measured and recorded for effective discrimination of significant and non-significant defects.

The present findings would appear to suggest that small numbers of large defects (as detected by the optimal prune criteria) are the dominant factor in determining WVTR.

Figure 7 Defects density: (a) defect density (all defects) and (b) significant defects count (see online version for colours)

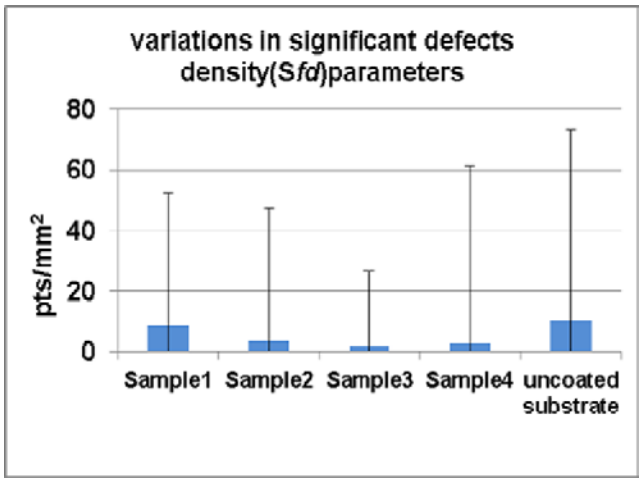

(a)

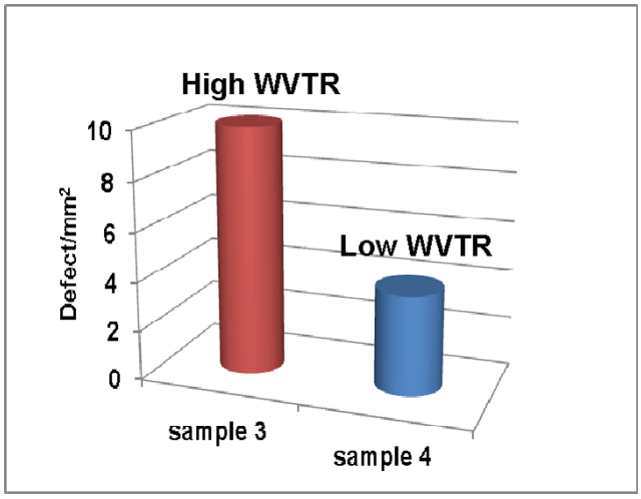

(b)

4.3 Scanning Electron Microscopy

The high lateral spatial resolution of ESEM imaging can provide information about defects in the Al_2O_3 barrier layer that are undetectable using optical interferometry or standard microscopy techniques. Imaging of the Al_2O_3 barrier layers was performed using a FEI Quanta 250 field emission gun environmental scanning electron microscope (FEG-ESEM). The spatial resolution of the instruments in environmental mode is approximately 1.4 nm at 30 keV when performing secondary electron imaging. To image the Al_2O_3/polymer structure low vacuum mode was employed using water vapour at pressures between 120–400 Pa. An off axis large field detector was used to collect the amplified secondary electron signal emitted from the specimen; this detector has the

advantage of providing images with a relatively large field-of-view. At these pressures charging effects are mitigated, thus allowing high contrast imaging of these electrically insulating samples to be undertaken without the need for a conductive surface coating. Elimination of the surface coating means the Al_2O_3 surface can be directly imaged, and no modification to the surface by the deposition of a conductive coating can be assured, which would be necessary using standard high vacuum mode SEM imaging.

An investigation of typical defects previously detected and catalogued by WLSI and optical microscopy was carried out in the ESEM, see Figure 8. A cross-sectional electron micrograph was collected near the edge of the Al_2O_3/polymer structure, see Figure 8(a). The image shows a 40 nm Al_2O_3 barrier layer which exhibits pit like defects between 100 nm to 500 nm in diameter on the surface. In Figure 8(b) an image of a typical hole defect approximately 4 µm in diameter in the Al_2O_3 layer is shown, a region of differing contrast is observed surrounding this hole; this is attributed to the delamination of the Al_2O_3 layer from the underlying polymer structure due to water penetration. The image shown in Figure 8(c) shows both micro-cracks and particulate on the surface of the barrier layer.

Figure 8 ESEM of defects in Al_2O_3 barrier layer: (a) Al_2O_3/polymer cross-section; (b) typical hole type defect and (c) micro-cracks and particulate

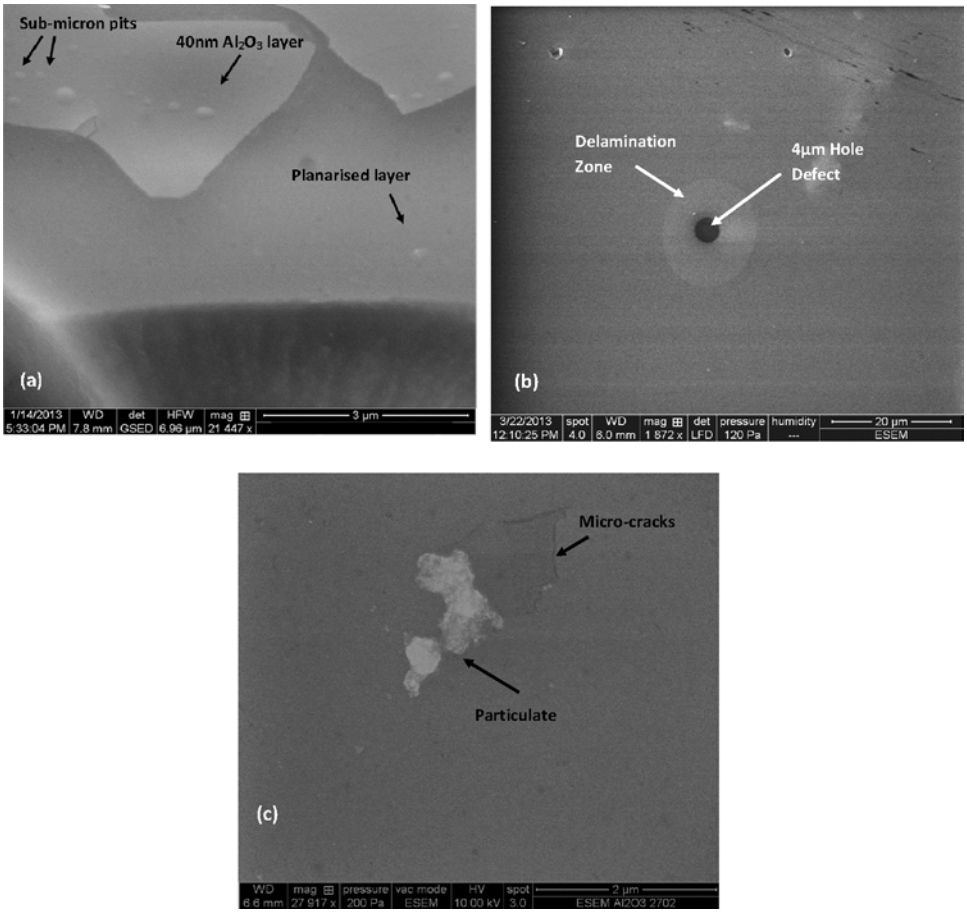

5 Conclusion

The Al_2O_3 barrier film is known to improve PV lifespan due to the reduction in WVTR. This improvement can be seriously affected and potentially reduced when defects in this barrier film are present. Surface metrology techniques have provided the ability to measure and effectively characterise these defects. The results provide new information that enables automatic defect detection methods to be developed. Information has also been provided on what type of defects will impede PV performance and lifespan. Feature segmentation analysis and the repeatability of the measurements have provided a clear evidence for the correlation of surface defects size, defect density, and the transmission of water vapour through the barrier coating layers. The investigation concludes that the total permeation rate corresponding to small numbers of larger defects is much greater compared to the total permeation rate corresponding to large numbers of small pinhole-type defects over the same area of substrate. This result provides important information which will be in valuable in the future development of an automatic in-line defect detection system and suggests that in-line inspection systems should concentrate on measuring the presence of 'large' defects rather than expending processing effort on trying to characterize large numbers of 'small' defects.

Acknowledgement

The authors would like to thank the EU for providing funds to carry out this work via the NanoMend project NMP4 LA-2011-280581.

References

Belyaev, A., Polupan, O., Dallas, W., Ostapenko, S. and Hess, D. (2006) 'Crack detection and analyses using resonance ultrasonic vibrations in full-size crystalline silicon wafers', *Applied Physics Letters*, Vol. 88, pp.1–3.

Carcia, P. F., McLean, R.S. and Hegedus, S. (2010b) 'Encapsulation of Cu(InGa)Se_2 solar cell with Al_2O_3 thin-film moisture barrier grown by atomic layer deposition', *Solar Energy Materials and Solar Cells*, Vol. 94, No. 12, pp.2375–2378.

Carcia, P.F., McLean, R.S. and Hegedus, S. (2010a) 'ALD moisture barrier for Cu (InGa)Se_2 solar cells', *ECS Transactions*, Vol. 33, No. 2, pp.237–243.

Connor, Z.M, Fine, M.E., Achenbach, J.D. and Seniw, M.E. (1998) 'Using scanning acoustic microscopy to study subsurface defects and crack propagation in materials', *Journal of Microscopy*, Vol. 50, No. 11.

Conroy, M. (2012) 'Use of interferometry for optimization of PV cell performance', *Metrology and Failure Analysis, Future Photovoltaics*, Taylor Hobson, UK, pp.1–5.

Duncan, B., Urquhart, J. and Roberts, S. (2005) *Review of Measurement and Modelling of Permeation and Diffusion in Polymers*, NPL Report DEPCR 012.

Florin, A. and Costin, C. (2011) 'Failure analysis capabilities for PV systems', *Recent Researchers in Energy, Environment, Entrepreneurship, Innovation*, Romania, pp.109–115, ISBN: 978-1-61804-001-5.

Hilmersson, C. (2006) *Detection of Cracks in Single-Crystalline Silicon Wafers Using Impact Testing*, A thesis submitted in partial fulfillment of the requirements for the degree of Master of Science in Mechanical Engineering, University of South Florida, South Florida.

ISO 25178-pt2 (2012) *Geometrical Product Specifications (GPS) – Surface Texture: Areal – Part 2: Terms, Definitions and Surface Texture Parameters*.

Jackson, P., Hariskos, D., Lotter, E., Paetel, S., Wuerz, R., Menner, R., Wischmann, W. and Powalla, M. (2011) 'New world record efficiency for Cu(In,Ga)Se2 thin-film solar cells beyond 20%', *Prog. Photovolt: Res. Appl*., Vol. 19, pp.894–897.

Jiang, X., Wang, K., Gao, F. and Muhamedsalih, H. (2010) 'Fast surface measurement using wavelength scanning interferometry with compensation of environmental noise', *Applied Optics*, Vol. 49, No. 15, May, p.2903.

Kempe, M. (2006) 'Modeling of rates of moisture ingress into photovoltaic modules', *Solar Energy Materials and & Solar Cells*, Vol. 90, No. 16, pp.2720–2738.

Olsen, L.C. (2010) *Barrier Coatings for Thin Film Solar Cells*, NREL/SR-52047582, Richland, Washington.

Rakotoniaina, J.P., Breitenstein, O., Al Rifai, M.H., Franke, D. and Schnieder, A. (2004) 'Detection of cracks in silicon wafers and solar cells by lock-in ultrasound thermography', *Proceedings of PV Solar Conference*, France, Paris.

Rueland, E., Herguth, A., Trummer, A., Wansleben, S. and Fath, B. (2005) 'µ-Crack detection and other optical characterisation techniques for in-line inspection of wafers and cells', *Proceedings 20th EU PVSEC*, Barcelona, pp.3242–3245.

Sander, M., Henke, B., Schweizer, S., Ebert, M. and Bagdahn, J. (2010) 'PV module defect detection by combination of mechanical and electrical analysis methods', *Photovoltaic Specialists Conference (PVSC), 2010 35th IEEE*, pp.001765, 001769.

Søndergaard, R., Hösel, M., Angmo, D., Thue, T., Olsen, L. and Krebs, F. (2012) 'Roll-to-roll fabrication of polymer solar cells', *Materials Today*, Vol. 15, pp.36–49.

Thein, M. (2006) *Atomic Layer Deposition (ALD)*, Available: A Tutorial by Cambridge NanoTech Inc., Cambridge, USA.